Analysis of Spatial-Spectral Relationships in Real Hyperspectral Imaging to use for Hyperspectral Unmixing.

Miguel A. Goenaga-Jimenez, Ph.D.[1], *Eduardo E. Castillo-Charris, Ph.D.*[1]
1Universidad del Turabo, Puerto Rico, mgoenaga1@suagm.edu, ecastillo@suagm.edu.

Abstract*– The basic statement on the linear unmixing model apply to hyperspectral images, is that the pixels are in the convex hull of the cone with the endmembers at its vertices. Hyperspectral data, in general, does not follow this structure. Here we use data exploration to analyze how spatial information can be used to extract uniform regions in the image. Several spectral unmixing algorithms look for a single convex region to depict a hyperspectral scene for a particular set of endmembers. A convex region can be defined in Euclidian space as if for every pair of points within the data cloud, every point on the straight-line segment that joins the pair of points is also within the data cloud. For instance, a solid cube is convex data cloud. This research proposes a methodology to perform unsupervised unmixing establishing how the spatial information help to capture the relationship between the grade of uniformity of the clusters, and the convex regions in the image data set. The effect of splitting the image helps us to obtain homogeneous regions. To achieve the localization of the endmember, principal component analysis is used, and the first three of them containing about 96% of the total information of hyperspectral image and then they are plotted for visualization their behavior. This analysis help us to understand the relation between the spatial domain information and data cloud structure. We saw experimentally that by partitioning the image in homogeneous regions we can decompose the data cloud in piece wise convex regions. We can then apply linear unmixing to these regions and easily extract endmembers for different homogeneous tiles in the image and shows how to perform hyperspectral unmixing using local information and merge them at a global level to develop an accurate description of the scene under study.

***Keywords*-- convex hull; hyperspectral Imaging Unmixing; spatial-spectral relationships; quadtree; principal components.**

Digital Object Identifier (DOI):
http://dx.doi.org/10.18687/LACCEI2017.1.1.411
ISBN: 978-0-9993443-0-9
ISSN: 2414-6390

Analysis of Spatial-Spectral Relationships in Real Hyperspectral Imaging to use for Hyperspectral Unmixing.

Miguel A. Goenaga-Jimenez, Ph.D.[1], Eduardo E. Castillo-Charris, Ph.D.[1]
[1]Universidad del Turabo, Puerto Rico, mgoenaga1@suagm.edu, ecastillo@suagm.edu.

Abstract– ***The basic statement on the linear unmixing model apply to hyperspectral images, is that the pixels are in the convex hull of the cone with the endmembers at its vertices. Hyperspectral data, in general, does not follow this structure. Here we use data exploration to analyze how spatial information can be used to extract uniform regions in the image. Several spectral unmixing algorithms look for a single convex region to depict a hyperspectral scene for a particular set of endmembers. A convex region can be defined in Euclidian space as if for every pair of points within the data cloud, every point on the straight-line segment that joins the pair of points is also within the data cloud. For instance, a solid cube is convex data cloud.***

This research proposes a methodology to perform unsupervised unmixing establishing how the spatial information help to capture the relationship between the grade of uniformity of the clusters, and the convex regions in the image data set. The effect of splitting the image helps us to obtain homogeneous regions. To achieve the localization of the endmember, principal component analysis is used, and the first three of them containing about 96% of the total information of hyperspectral image and then they are plotted for visualization their behavior.

This analysis help us to understand the relation between the spatial domain information and data cloud structure. We saw experimentally that by partitioning the image in homogeneous regions we can decompose the data cloud in piece wise convex regions. We can then apply linear unmixing to these regions and easily extract endmembers for different homogeneous tiles in the image and shows how to perform hyperspectral unmixing using local information and merge them at a global level to develop an accurate description of the scene under study.

Keywords-- convex hull; hyperspectral Imaging Unmixing; spatial-spectral relationships; quadtree; principal components.

I. INTRODUCTION

In hyperspectral imaging, the reflected radiation characterized by a specific pixel in the remotely sensed image not often comes from the interaction with an only one homogeneous material. Though, the extraordinary spectral resolution of imaging spectrometers allows the recognition, and classification of subpixel materials from their contribution to the measured spectral signal. The unmixing is a hyperspectral image processing approach for subpixel information extraction, where the measured spectral signature is decomposed into a collection of fundamental spectra, or endmembers, and a set of corresponding portions or abundances which correspond to the fractional area occupied by the specific endmember in that pixel.

Digital Object Identifier (DOI): http://dx.doi.org/10.18687/LACCEI2017.1.1.411
ISBN: 978-0-9993443-0-9
ISSN: 2414-6390

The use of only one endmember, to represent an endmember class does not take into account the variability of spectral signatures caused by natural factors. For instance, in a rocky scene, the spectral signature of a particular kind of mineral may vary due to mixing soil or by water content. Simple spectral mixture analysis (SSMA) can, by itself, provide suitable accuracies in some relatively homogeneous environments, but because of the spectral complexity of many landscapes, the use of fixed endmember spectra may results in inaccurate unmixing analysis for complex regions over wide landscapes [1].

The effect of splitting the image using quadtree region partitioning, helps us to obtain homogeneous regions. To achieve the localization of the endmember, principal component analysis is used, the first three of them containing about 96% of the total information of hyperspectral image and then they are plotted for visualization. For endmember extraction, we proposed to extract local endmembers in each quadtree region, and merge them at a global level to develop an accurate description of the scene under study

This paper show an approach that perform unsupervised unmixing where endmember classes are assumed to be composed of multiple spectral endmembers to look at local information as a result to use region partitioning method starting with the hypothesis that to split the image help us to obtain convex and homogeneous regions in the image.

II. BACKGROUND

A. Linear Mixing Model

In hyperspectral imaging, the reflected or emitted radiation represented by a single pixel in the remotely sensed image rarely comes from the interaction with a single homogeneous material. However, the high spectral resolution of imaging spectrometers enables the detection, identification, and classification of sub-pixel objects from their contribution to the measured spectral signal. The linear mixing model [1] [2] represents a pixel as the linear combination of the spectral signatures of each material multiplied by its fractional coverage area or abundance.

$$\boldsymbol{x}_j = \sum_{i=1}^{p} \mathbf{s}_i \mathbf{a}_i + \boldsymbol{w} = \mathbf{S}\mathbf{a}_j + \mathbf{w}_j \quad j = 1,2,3,\ldots,N \tag{1}$$

where $x_j \in \Re_+^m$ is the measured spectral signature at pixel, $S \in \Re_+^{m \times p}$ is the endmembers matrix, $a_j \in \Re_+^p$ is the spectral abundances vector, and $w_j \in \Re_+^m$ is a measurement noise vector, *m* is the number of spectral bands, and *p* is the number of endmembers. In HSI, *m* >> *p*, notice that all elements of ***S***, ***a***, and ***x*** are constrained to be positive, and the sum of a_{ij} for all spectral bands *m* is less than or equal to one. For the full HSI, the linear mixing model (1) can be written in matrix form as:

$$\mathbf{X} = \mathbf{SA} + \mathbf{W} \tag{2}$$

where **X** = [x_1 ... x_N] is the matrix containing all image pixels, **S** = [s_1 ... s_p] is the matrix of endmembers, **A** = [$\mathbf{a}_1$ ... $\mathbf{a}_N$] is the matrix of abundances, **W** = [w_1 ...w_N] is the noise matrix, and N is the number of pixels in the image.

B. Spectral Unmixing

Spectral unmixing is the inverse procedure where given the image X, we want to determine the number of endmembers p, the endmember matrix S, and the abundance matrix A.

Mathematically, the unmixing problem could be stated as follows:

$$(\hat{\mathbf{p}}, \hat{\mathbf{S}}, \hat{\mathbf{A}}) = \arg\min_{\mathbf{S}_{ij}>0, \mathbf{A}_{ij}>0, \sum_{i=1}^{p} a_i \leq 1, p \in Z} \left\|\mathbf{X} - \mathbf{SA}\right\|_{\mathbf{F}}^2 \tag{3}$$

where || ||F is the Frobenious norm. The optimization problem in (3) is related to a constrained non negative matrix factorization (cNMF) [3]. If the number of endmembers and the endmember matrix S were known in (3), the problem becomes the abundance estimation problem which is a constrained linear least squares problem. The fully constrained abundance estimation problem has been solved using different approaches. See for instance [4][8].

Different approaches have been proposed to solve the linear unmixing problem. Most state of the art methods solve the unmixing problem in two stages and not as an optimization problem like (3). In the first stage, the number of endmembers is determined and spectral signatures of the endmembers are extracted by searching for "pure" pixels in the image by using spectral signatures from a library or from field data [1] [2]. In the second stage, abundances are estimated.

C. Endmember Extraction Approaches

Once the number of endmember is estimated, the next step is to find the endmember signatures. Most algorithms assume that endmembers are known a priori. Spectral libraries obtained in laboratories or collected in the field can be used as endmembers, but automated unmixing algorithms seek to extract the endmember signatures from the hyperspectral image itself.

Most of unmixing algorithms are pixel-to-pixel techniques that do not take into account the spatial information captured in hyperspectral imaging. Some unmixing algorithms that use the spatial and spectral information have been introduced recently [7].

Automated unmixing algorithms can be classified in Geometric, Parametric and Spatial Spectral Algorithms.

D. Geometric Approaches

Algorithms based on geometric models assume that pixels are enclosed in a simplex whose corners are the endmembers. The geometrical mixing model provides an intuitive mean to describe the endmember determination problem which is reduced to determining the corners of the minimum volume simplex that encloses the data cloud [1], [2]. Figure 1 shows examples of simplex.

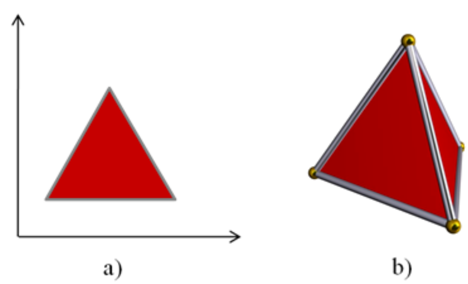

Fig. 1 Simplex illustration in (a) 2-D and (b) A regular 3-D simplex or tetrahedron.

The relation between the unmixing problem and convex geometry has been used by many researchers to develop algorithms for the extraction of endmember signatures. Some examples of the most used geometric methods are Pixel purity index, N-Finder, Maximum Distance (MaxD), Vertex Component Analysis (VCA) and Nonnegative Matrix Factorization (NMF) [9] [10]. In this approach is used the NMF method.

E. Endmember Classes

In hyperspectral image classification, information classes are related with categories of interest to the user, while spectral classes refer to pixels with similar spectral signatures [11]. An information class may be composed of several spectral classes [13]. It is unusual to find several spectral classes for the same soil information class, for the same apparent type of vegetation, and so on for other cover types in a scene. These variances may result from alterations in wetness content, earth type, topographic effects, among others.

Endmember classes are defined in similar way to information classes. Using a single spectral signature to represent an endmember class does not take into account the variability of these spectral signatures; hence, it is more natural to talk about multiple spectra representation of an endmember or an endmember class. In our approach, a single endmember spectral signature will play the role of a spectral class in classification.

To develop an approach to unsupervised unmixing in large scene images, we propose to look at local tiles to extract local spectral endmembers. We expect that at a local level there are more homogeneous conditions, which may allow description of an endmember class by a single spectrum. Once local endmember are extracted, they are combined to extract endmember classes for global descriptions of the scenes.

F. Abundance Estimation

Once the endmembers are determined, the next step is to estimate their abundances. Abundance estimation is the process (AEP) of determining the abundances associated with the endmembers for each pixel in the image. The AEP for a particular pixel x_j is given by the constrained linear least squares problem [5] [6]:

$$\bar{a} = \arg\min_{a_{ij}\geq 0, \sum_{i=1}^{p} a_i = 1} \left\| \mathbf{x}_j - \mathbf{S}\,\mathbf{a}_j \right\|_2^2 \tag{4}$$

The objective function in (4) and constraints are convex, consequently the solution is unique. Several solution methods have been proposed in the literature for (4), [5, and 6].

G. Quadtree Partitioning

Quadtree is unbalanced spatial data structure made by recursive partitions of space in four equals size quadrants. This spatial data structure is used commonly for represent an image in numerous applications, like content-based image retrieval and compressing images. Moreover, it is used in computer graphics, image processing, and Geographical Information Systems (GIS).

Different types of data can be represented by quadtree data structure [18], the most known quadtree is called "region quadtree", let us cutting an image in regions or quadrants according to a given split criterion. Then, the quadtree help us to represent images at different levels of homogeneity (Fig. 2) [13].

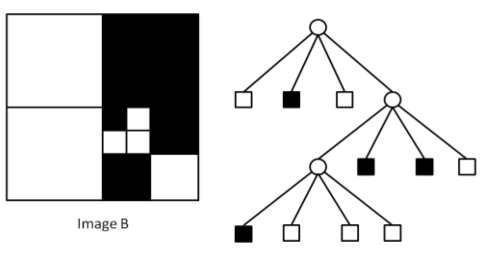

Fig. 2 Synthetic binary image and the region quadtree representation.

III. Procedure

The proposed procedure consists of several steps that are mentioned bellow:

A. Spatial Partitioning

The process start with the determination of the appropriate number and size of the spatial subsets for a specific image. This is perform calculating the split criterion to estimate the grade of homogeneity of the portion of the image. Several metrics are used to obtain it (mean distance from the spectral centroid, norm of the spectral centroid, mean of all values in the image, norm of Shannon entropy) [15] [16].

B. Local Endmember Extraction

The endmember extraction is performed on each portion of the image. The non-negative matrix factorization algorithm of [4] is used to extract endmembers. Non-Negative Matrix Factorization (NMF) approximation based algorithms [4] [5] [7] do not assume that there are pure pixels in the image, which is very important for low spatial resolution images. Given the number of endmembers *p*, the NMF determines the endmember matrix $\hat{\mathbf{S}}$ and abundance matrix $\hat{\mathbf{A}}$ by solving the optimization problem:

$$\hat{\mathbf{S}}, \hat{\mathbf{A}} = \mathbf{arg\,min}_{\mathbf{S}_{ij}>0, \mathbf{A}_{ij}>0, \sum_{i=1}^{p} a_i = 1} \left\| \mathbf{X} - \mathbf{SA} \right\|_F^2 \tag{9}$$

where $\| \ \|_F$ is the Frobenious norm.

C. Finding Endmember Classes

Once endmembers for each spatial subset are extracted, the next step is to combine them into endmembers classes. Clustering methods are being exploited to extract the endmember classes [17][18]. Spectral endmembers are clustered using the angle distance. In the experiments, endmember classes were built using the cosine of spectral angle distances with threshold of 99%. Improving the extraction of endmember classes was made applying segmentation methods for more accuracy.

D. Global Abundance Estimation

With the endmember classes selected, the next step is to extract their abundances. Abundances are computed using the same approach (NMF) of the equation (4). All extracted signatures are used for computing abundances. The abundance of an endmember class is the sum of the abundances for the spectral signatures in that class. Constrained least squares (4) or sparse regression are used to compute the abundance depending on whether or not there are more spectral endmember than bands [4][5].

E. Hyperspectral Data

In the experiments presented here, the 30-m spatial resolution AVIRIS image collected over Fort A.P. Hill in Virginia (see Fig. 3) is used. A classification map from [13] [20] is also shown in Fig. 3 depicting the different classes in the image. This thematic map is used to evaluate how well the proposed approach extracts individual information classes in the image.

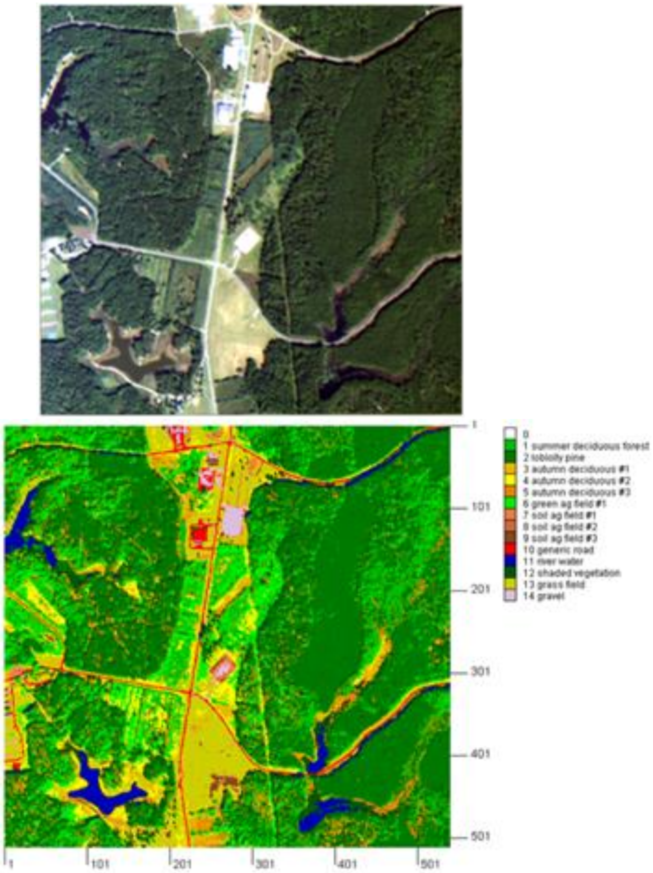

Fig. 3 True color composite and classification map for AVIRIS image from Fort A.P. Hill AFB, VA [19].

IV. Experimental Results

After the image is partitioning the results obtained using the Shannon Entropy as a split criterion the partition are show at the following Figure 4.

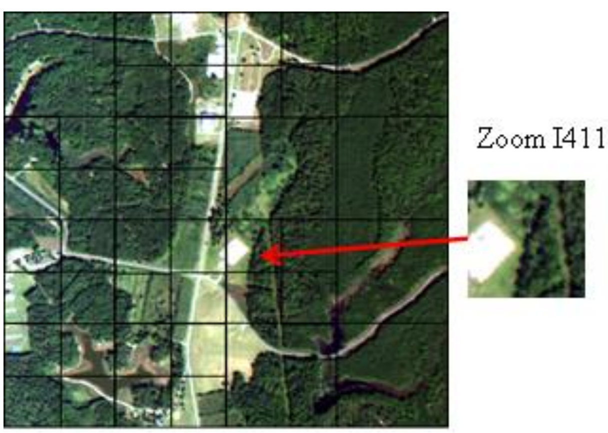

Fig. 4 Partitions using norm of the Shannon Entropy

Selecting the specific tile ZoomI411 of the Fig. 4 we can see the pixel distribution in the tile for a real hyperspectral image. The data is processed applying a principal component analysis (PCA) and select the three first PCA that contains around of 96% of the information of the all data. Using these three first PCA of the data the we can visualize the data using scatterplots in three dimension using MATLAB.

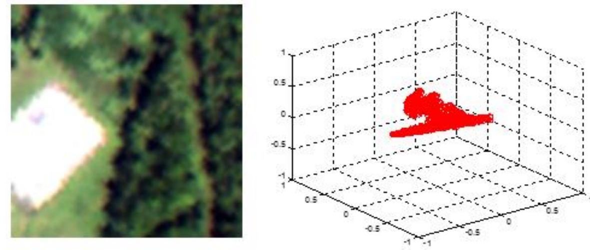

Fig. 5 Partitions using norm of the Shannon Entropy

As mention above the basic assumption on the linear unmixing model is that the pixels are in the convex hull of the cone with the endmembers at its vertices. But, real hyperspectral data in general does not follow the structure as shown in the Fig. 5. Here we use exploratory data analysis to analyze how spatial information can be used to extract homogeneous regions in the image.

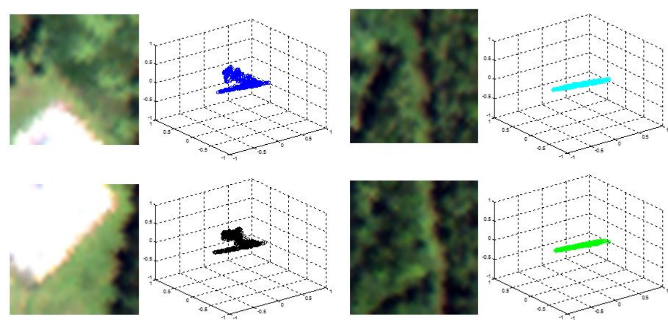

Fig. 6 Quadtree partitions using norm of the Shannon Entropy in fig. 5.

As shown in Fig. 6 at right, although there are still distinguishable classes on the image, its data cloud is convex, the data cloud shows an elongated convex form that represent 2 endmembers which clearly facilitates endmember extraction and unmixing. Fig. 6 at left include the buildings class and still shows a non-convex data cloud. Notice that the image is not a uniform sub-tile of the image. If the division process is repeated with the top left image.

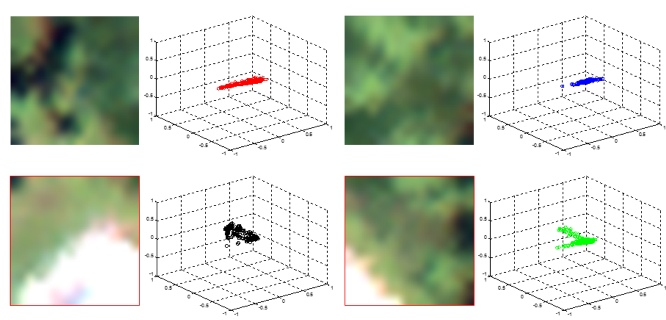

Fig. 7 Quadtree partition using norm of the Shannon Entropy from part top left of fig. 6.

Then when we repeat the procedure again, zoom top left of the Fig. 6 is partitioned into four quadrants as shown in Fig. 7, notice that the tiles show different levels of uniformity, emerging new convex hull at the data cloud. Again, uniform tiles lead to convex data clouds and in the lower right image show non-uniform tiles and, hence non-convex data clouds. These results suggest that by decomposing the image in homogeneous regions, we partition its data cloud into piece wise convex regions. This is the main motivation behind image partitioning. Using this trend, by dividing the image we establish easier the spectral signatures of different materials found in the image. The image is processed to obtain 148 endmembers throughout the all global image, that to be grouped into eleven different endmember classes.

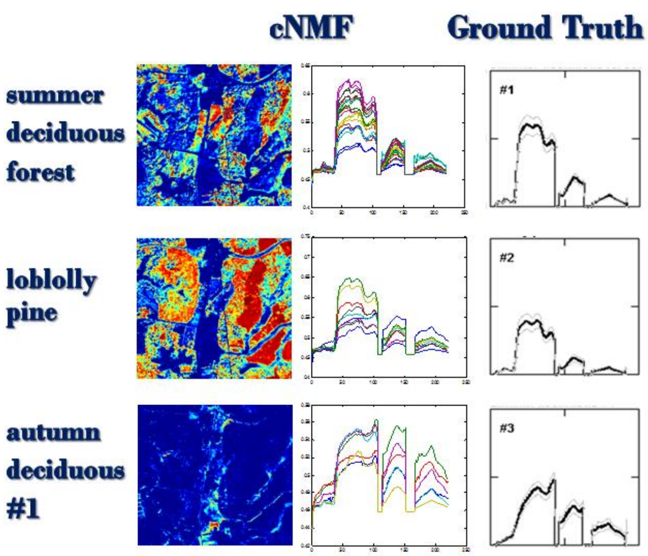

Fig. 8 Results obtained for endmember classes of summer deciduous forest, loblolly pine and autumn deciduous #1.

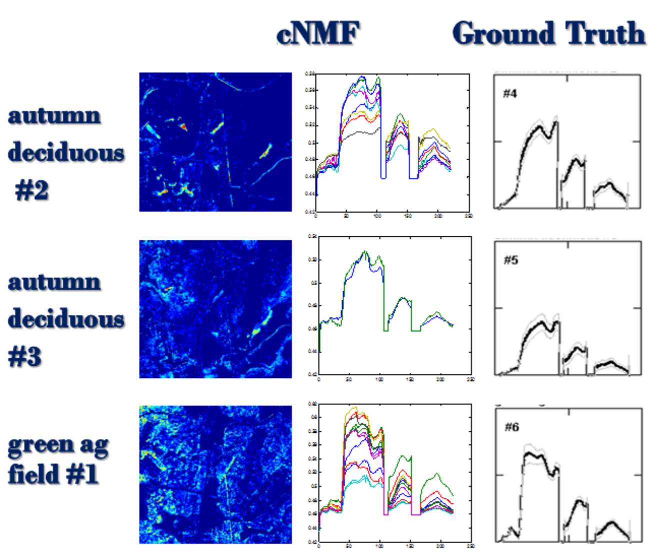

Fig. 9 Results obtained for endmember classes of autumn deciduous #2, autumn deciduous #3 and green ag field #1.

With these unmixing results we saw experimentally that by partitioning the image in homogeneous regions we can decompose the data cloud in piece wise convex regions. Then we can apply linear unmixing to these regions and easily extract endmembers for different homogeneous tiles in the image.

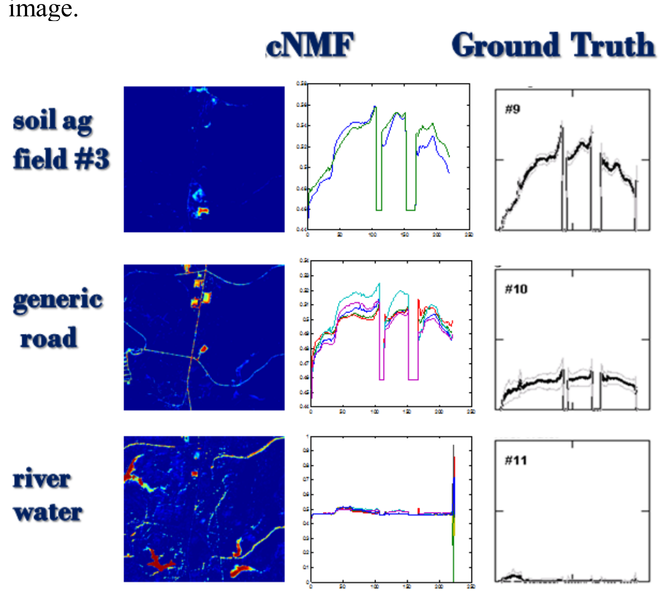

Fig. 10 Results obtained for endmember classes of soil ag field #3, generic road and river water.

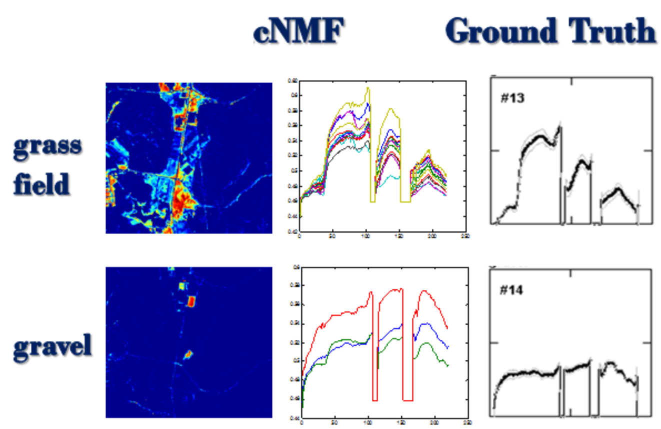

Fig. 11 Results obtained for endmember classes of grass field and gravel.

Finally, we understand the relation between the spatial domain information and data cloud structure. Also, using the exploratory data analysis to analyze how spatial information can be used to extract homogeneous regions in the image to be more accuracy the extraction the endmember of the different material in the image.

The table 6-1 show the results of the classifications of the different classes for the AP-Hill image compared with the given ground true. The classes, summer deciduous, loblolly pine, soil ag field, river water, grass field and gravel had a good result in the classification around 86.23% that is like the overall performance of the classification in the entire image, because there are the majority classes in the image. The total pixels in this image was 262,144 and the highest percent of the detection were the grass field with 96.75%, and the river water 95.38%, and the lowest percent were the generic road with 59.67% and the shaded vegetation with 65.58%.

TABLE I
CONFUSION MATRIX FOR THE APHILL IMAGE.

APHill Image											
Overall Accuracy:		86.46%									
Kappa Coefficient:		0.496									
Class	**1**	**2**	**3,4,5**	**6**	**7, 8, 9**	**10**	**11**	**12**	**13**	**14**	**Total**
1	86920	7436	142	2652	12	4	76	89	8	2	97341
2	9123	53284	76	1350	18	8	84	142	5	3	64093
3, 4, 5	1120	89	7001	2130	320	34	62	560	620	12	11948
6	1525	834	45	10957	3	5	2	5	8	2	13386
7, 8, 9	5	9	68	15	7449	2	16	18	356	2	7940
10	0	3	17	2	2	4136	13	20	967	7	5167
11	83	6	9	21	10	2	14909	365	3	1	15409
12	1624	863	460	896	128	12	18	11210	32	15	15258
13	142	12	231	274	83	2	0	0	25362	7	26113
14	10	8	17	8	2	1	11	0	0	5432	5489
Total	100552	62544	8066	18305	8027	4206	15191	12409	27361	5483	262144

V. Conclusions

The experimental results showed the potential of the proposed approach to perform unsupervised unmixing of large scenes images, and to extract spectral endmember classes that better capture the spectral variability in an endmember class. By decomposing the image into uniform regions and extracting endmembers for each tile using cNMF we make the cNMF sensitive to spatial information.

The exploratory data analysis of the behaviour of the data cloud in the image to demonstrate how the spatial information help to capture the relationship between the grade of uniformity, clusters, and the convex regions in the image data set helping to improve the hyperspectral unmixing process. Looking for homogeneous regions in the scene, guarantee that when we perform spectral unmixing in each partition, will be working regions of data that can be enclosed in convex regions.

Breaking the large scene into tiles allowed the extraction of spectral endmember classes that had small contrast at the full image level but high contrast at the local level. Several issues still need to be addressed, in particular, how to select the optimal tile size and faster ways to determine the number of endmembers.

Results from the local unmixing analysis agree more with published ground truth for the A.P. Hill image than what was possible with the global approach. This is encouraging since the proposed method was fully image based with some analyst intervention for endmember class tuning.

Acknowledgment

The facilities of the Center for Subsurface Imaging Systems (CenSSIS) in the UPR at Mayaguez and Turabo University at Gurabo Campus.

References

[1] Keshava, N. and Mustard, J.F. "Spectral unmixing". Signal Processing Magazine, IEEE, 19(1):44-57, Jan 2002.

[2] Keshava, N. "A Survey of Spectral Unmixing Algorithms". In Lincoln Laboratory Journal, 2003. Volume: 14. Number 1, Page(s): 55 - 78, April 2003.

[3] Jia, S. and Qian, Y. "Constrained nonnegative matrix factorization for hyperspectral unmixing". Geoscience and Remote Sensing, IEEE Transactions on, 47(1):161 - 173, January. 2009.

[4] Masalmah, Y. M. and Vélez-Reyes, M. "A full algorithm to compute the constrained positive matrix factorization and its application in unsupervised unmixing of hyperspectral imagery". In Sylvia S. Shen and Paul E. Lewis, editors, Algorithms and Technologies for Multispectral, Hyperspectral, and Ultraspectral Imagery XIV, volume 6966, page 69661C. SPIE, 2008.

[5] Vélez-Reyes, M. and Rosario, S. "Solving abundance estimation in hyperspectral unmixing as a least distance problem". In Geoscience and Remote Sensing Symposium, 2004. IGARSS '04. Proceedings. 2004 IEEE International, volume 5, pages 3276 -3278 vol.5, Sept. 2004.

[6] Chang, C., & Ji, B. "Weighted abundance-constrained linear spectral mixture analysis". IEEE Transactions on Geoscience and Remote Sensing, 44, 378−388. 2006.

[7] Chang, C., Du, Q. "Estimation of number of spectrally distinct signal sources in Hyperspectral Imagery". IEEE Transactions on Geoscience and remote sensing, Vol.42(3), Page(s): 608-619, March 2004.

[8] Masalmah, Y. and Vélez-Reyes, M. "Unsupervised Unmixing of Hyperspectral Imagery". 49th IEEE International Midwest Symposium on Circuits and Systems (MWSCAS'06). Volume: 2. Page(s): 337 - 341, October, 2006.

[9] Parente, M., and Plaza, A. "Survey of Geometric and Statistical Unmixing Algorithms for Hyperspectral Images". Geoscience and Remote Sensing Symposium (IGARSS), 2011 IEEE International, July 24-29. Pages: 1135−1138. 2011.

[10] Bioucas-Dias, J., and Plaza, A. "An Overview on Hyperspectral Unmixing: Geometrical Statistical, and Sparse regression based Approaches". Hyperspectral Image and Signal Processing: Evolution in Remote Sensing (WHISPERS), 2010 2nd Workshop on, June 14-16. Pages: 1−4. 2010.

[11] Goenaga-Jimenez M., Vélez-Reyes, M. “Integrating spatial information in unmixing using the nonnegative matrix factorization”. SPIE Proceedings Volume 9088: Algorithms and Technologies for Multispectral, Hyperspectral, and Ultraspectral Imagery XX, July 2014.

[12] Richards, J. A. and Jia, X. "Remote sensing digital image analysis: An Introduction". Berlin: Springer, English Version: 4th Ed.2006.

[13] Goenaga-Jimenez M., Vélez-Reyes, M. “Comparing Quadtree Region Partitioning Metrics for Hyperspectral Unmixing”. SPIE Proceedings Volume 8743: Algorithms and Technologies for Multispectral, Hyperspectral, and Ultraspectral Imagery XX, June 2013

[14] Roberts, D. A., Gardner, M., Church, R., Ustin, S., Scheer, G., & Green, R. O. "Mapping Chaparral in the Santa Monica Mountains Using Multiple Endmember Spectral Mixture Models". Remote Sensing of Environment, 65, 267−279. 1998.

[15] M. A. Goenaga, M. C. Torres-Madronero, M. Velez-Reyes, S. J. Van Bloem and J. D. Chinea. “Unmixing Analysis of a Time Series of Hyperion Images Over the Guánica Dry Forest in Puerto Rico,” in IEEE Journal of Selected Topics in Applied Earth Observations and Remote Sensing, vol. 6, no. 2, pp. 329-338, April 2013.

[16] Lobell, D. B., Asner, G. P., Law, B. E., & Treuhaft, R. N. "View angle effects on canopy reflectance and spectral mixture analysis of coniferous forests using AVIRIS". International Journal of Remote Sensing, 23, 2247−2262. (2002).

[17] Bateson, C. A., Asner, G. P., & Wessman, C. A. "Endmember bundles: A new approach to incorporating endmember variability into spectral mixture analysis". IEEE transactions on geoscience and remote sensing, 38, 1083−1094. 2000.

[18] Goenaga-Jimenez M., Vélez-Reyes, M. “Incorporating Local Information in Unsupervised Hyperspectral Unmixing”. SPIE Proceedings Volume 8390: Algorithms and Technologies for Multispectral, Hyperspectral, and Ultraspectral Imagery XX, June 2012

[19] Rogge, D. M., Rivard, B., Zhang, J., Sanchez, A., Harris, J., Feng. "Integration of spatial and spectral information for the improved extraction of endmembers". Remote Sensing of Environment, 110, 287−303. 2007

[20] Cipar, J., Lockwood, R., Cooley, T., Grigsby, P. “Background Spectral Library for Northeastern Virginia”. AVIRIS Workshop. 2003.